

# Therapeutic luminal coating of the intestine

Yuhan Lee<sup>1,6\*</sup>, Tara E. Deelman<sup>2,3,4,6</sup>, Keyue Chen<sup>1</sup>, Dawn S. Y. Lin<sup>1</sup>, Ali Tavakkoli<sup>2,4,5\*</sup>  
and Jeffrey M. Karp<sup>1\*</sup>

**The gastrointestinal tract is the site of most drug delivery and therapeutic interventions for the management and treatment of numerous diseases. However, selective access to its mucosa, especially in the small bowel, is challenging. Here we develop an orally administered gut-coating formulation that provides a transient coating of the bowel. Through a materials screening campaign, we identified a sucrose octasulfate aluminium complex and further engineered the pH-dependent material into a complex coacervate formulation linked via pH-independent electrostatic interaction, which allowed an effective transient physical coating on the gastrointestinal mucosa, independent of gastric acid exposure. We tested the therapeutic values of this technology in two settings. Oral administration of this gut-coating formulation modulated the nutrient contact with bowel mucosa, which lowered the glucose responses in rodent models indicating a potential therapeutic utility in diabetes. Furthermore, the formulation protected biological agents from gastric acid exposure and degradation, which enabled oral delivery to the small bowel mucosa.**

The gastrointestinal tract, specifically the small bowel, is not only the principal site of nutrient digestion and absorption, but also one of the body's largest reservoirs of immunologically active and hormone-producing cells. As such, the intestine has been increasingly recognized as critical to the pathogenesis of systemic diseases, and substantial data highlights the role of the small bowel as a therapeutic target for local and systemic diseases. The most notable of these observations are data that support the role of the small intestine as a therapeutic target in type-2 diabetes (T2D)<sup>1–4</sup>. The Roux-en-Y gastric bypass (RYGB) is one of the most commonly performed weight-loss procedures in United States and the world. The surgery both creates a new 30–60 cm<sup>3</sup> volume gastric pouch, and bypasses a significant portion of the stomach and the proximal small intestine<sup>1–5</sup>. Most markedly, obese type-2 diabetes mellitus patients who undergo RYGB surgery experience an early and weight-independent improvement or complete resolution of their T2D<sup>3,5–7</sup>. Furthermore, many well-known diseases, such as inflammatory bowel disease (IBD), affect the mucosal surface of the bowel, yet direct localized drug delivery to the affected mucosa is challenging. For the purposes of topical delivery of biologics to the distal small bowel, which is often the affected site in patients with IBD, the main obstacles include high gastric acidity and low pH, and proteolytic gut enzymes<sup>8,9</sup>. Although there have been approaches to overcome each challenge, the bioavailability of protein drugs delivered through an oral route remains too low<sup>9,10</sup>. As a result, these agents are given systemically, which increases their cost as well as side effects. Drug delivery systems that can directly deliver drugs to the targeted regions of the gut with minimal systemic exposure provide significant advantages, which include prolonged drug efficacy, lowered dosing frequency and decreased side effects. These diverse observations highlight the critical need to develop a therapeutic platform technology that can provide reliable access to the small bowel mucosa.

Here we describe the development of an orally delivered therapeutic platform that forms a transient physical coating on the bowel (Fig. 1a). To identify potential coating materials that are safe, we screened candidate materials on the US Food and Drug Administration's (FDA's) generally recognized as safe list and materials that exist in FDA-approved products that are orally administered. Materials placed on a mucin-coated porous cellulose nitrate membrane were first subjected to gravitational loading followed by permeability testing of an acidic D-glucose solution in simulated stomach acid (120 g l<sup>-1</sup>, pH 1.0) (Fig. 1b). Glucose was selected as a primary target due to our interest in T2D. The most-effective barrier properties to glucose permeation were achieved for gum karaya (65% blocked), sucrose octasulfate aluminium complex (sucralfate) (62% blocked), methylcellulose (60% blocked) and pectins (45% blocked for pectin from citrus, 44% blocked for pectin from apples) (Fig. 1c). To assess how the barrier properties change over time, the best eight of the performing materials were selected for further testing. Although materials such as methylcellulose and pectins showed similar blocking properties compared to sucralfate during a permeation test, they quickly dissolved within the glucose solution, whereas sucralfate maintained its sticky paste structure (Fig. 1d,e). Compared to the other materials tested that only transiently achieved effective barrier properties, sucralfate formed a stable coating on the mucin-coated surface and maintained a substantial barrier effect for several hours (Supplementary Fig. 1).

Although sucralfate showed excellent barrier function in the *in vitro* screening study in which candidate materials were formed on the simulated mucosal surface, sucralfate is a pH-dependent material that only forms the sticky paste in an acidic environment (for example, in stomach acid) and selectively binds to ulcerated mucosa where bicarbonate secretion malfunctions (that is, acidic). On healthy bicarbonate-neutralized mucosa with pH higher than that of stomach acid, sucralfate forms loosely bound discrete solid aggregates rather than a continuous layer (Fig. 2a)<sup>11–13</sup>. When

<sup>1</sup>Engineering in Medicine, Department of Medicine, Center for Regenerative Therapeutics, Brigham and Women's Hospital, Harvard Medical School, Harvard Stem Cell Institute, Harvard-MIT, Division of Health Sciences and Technology, Boston, MA, USA. <sup>2</sup>Department of Surgery, Brigham and Women's Hospital, Harvard Medical School, Boston, MA, USA. <sup>3</sup>Department of Surgery, Erasmus MC University Medical Center, Rotterdam, the Netherlands. <sup>4</sup>Laboratory for Surgical and Metabolic Research, Brigham and Women's Hospital, Harvard Medical School, Boston, MA, USA. <sup>5</sup>Center for Weight Management and Metabolic Surgery, Brigham and Women's Hospital, Harvard Medical School, Boston, MA, USA. <sup>6</sup>These authors contributed equally: Yuhan Lee, Tara E. Deelman. \*e-mail: [ylee21@bwh.harvard.edu](mailto:ylee21@bwh.harvard.edu); [atavakkoli@bwh.harvard.edu](mailto:atavakkoli@bwh.harvard.edu); [jeffkarp@bwh.harvard.edu](mailto:jeffkarp@bwh.harvard.edu)

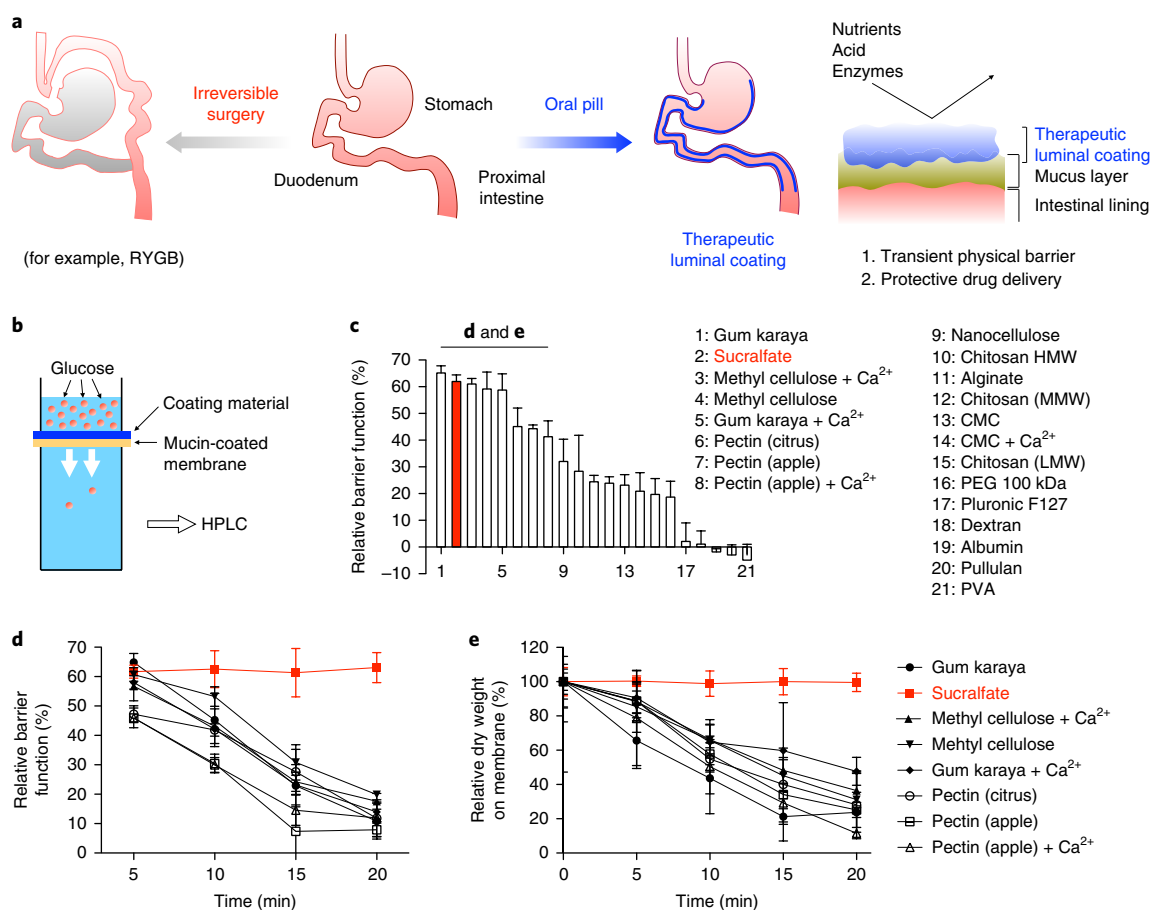


**Fig. 1 | Therapeutic coating of the gastrointestinal tract via an orally administered formulation and in vitro screening of the candidate intestine coating materials.** **a**, The illustration demonstrates the oral administration luminal coating of the intestine as an alternative to highly invasive and irreversible bariatric surgeries (for example, RYGB). The coating is designed to form a transient physical barrier on mucosa against substances such as nutrients, acids and enzymes, and a drug delivery platform that can deliver therapeutics (for example, protein) protected from stomach acid and digestive enzymes. **b**, Schematic representation of the integrative permeation test. Briefly, a solution of the candidate material is applied to a mucin-coated porous membrane, vertically tilted for 1 min and then mounted in a Franz cell apparatus, and glucose permeation is then measured using HPLC. **c**, Screening results of the candidate intestine coating materials. Gum karaya, sucralfate, methylcellulose and pectins exhibited the most-effective barrier properties and were further examined for their stability over time. CMC, carboxymethylcellulose; PVA, poly(vinyl alcohol). **d**, Integrative barrier function kinetics of the best materials identified from the screen (1–8 in **c**). Sucralfate formed the most stable barrier on mucus-coated surfaces. **e**, Dry-weight change over time for selected materials (1–8 in **c**) attached to mucin-coated membranes. The dry weight of sucralfate remained unchanged for at least 20 min. HMW, high molecular weight; MMW, medium molecular weight; LMW, low molecular weight.

healthy (that is, non-ulcerative) Sprague Dawley (SD) rats were gavaged with sucralfate, computed tomography (CT) images and fluorescent microscopy images showed that sucralfate was sparsely scattered in the stomach and intestine in low density and washed out in a few hours (Fig. 2b,c and Supplementary Movies 1 and 2), probably because of the change in rheological properties. When acidified sucralfate paste in simulated stomach acid (pH 1.0) was added to higher pH solutions, the phase angle ( $\delta$ ), the measure of the presence of solid behaviour in a viscoelastic fluid in oscillatory rheological analysis, gradually decreased, which indicates the formation of weak solid aggregates (Fig. 2d). Furthermore, when sucralfate was applied on a mucus-coated membrane in pH 1.0 and transferred to solutions with higher pH (>2.0), the barrier function steeply decreased (only ~16.5% glucose blocked at pH 4.0) (Fig. 2e). As a result, when healthy SD rats, pretreated with sucralfate, were subjected to oral glucose tolerance tests (OGTTs), the peak glucose values were similar to controls at all time points (Fig. 2f) and there was no significant difference in the incremental area under the curve (iAUC) between sucralfate and saline-treated groups

(Fig. 2g). These results suggest that further engineering of sucralfate is required to maximize the binding affinity on healthy mucosa and its ability to form a barrier to nutrient absorption.

Sucralfate is a water-insoluble salt that comprises two oppositely charged polyelectrolytes: anionic sucrose octasulfate and a high molecular weight cationic polyaluminium complex (PAC) (Fig. 3a)<sup>14,15</sup>. PAC is a cationic inorganic polymer with aluminium as a backbone linked together via coordination bonds with hydroxy linkages ( $-\text{OH}-$ ) (ref. 16). When PAC is exposed to stomach acid, the hydroxy linkages are reversibly protonated to give  $-\text{OH}_2^+$  linkages to form a sticky paste combined with sucrose octasulfate. However, with increasing pH, the hydroxyl linkages in PACs are deprotonated to form a solid (Fig. 2). Therefore, we hypothesized that to convert the sucralfate into a complex coacervate system by irreversibly converting the hydroxyl linkages into bound water ( $-\text{OH}_2$ ) could eliminate sucralfate's pH dependency to form a sticky paste and thus could effectively coat all regions of the gastrointestinal tract without the need for stomach acid (Fig. 3a). Furthermore, the resultant bound water could be reversibly dehydrated/hydrated to formulate

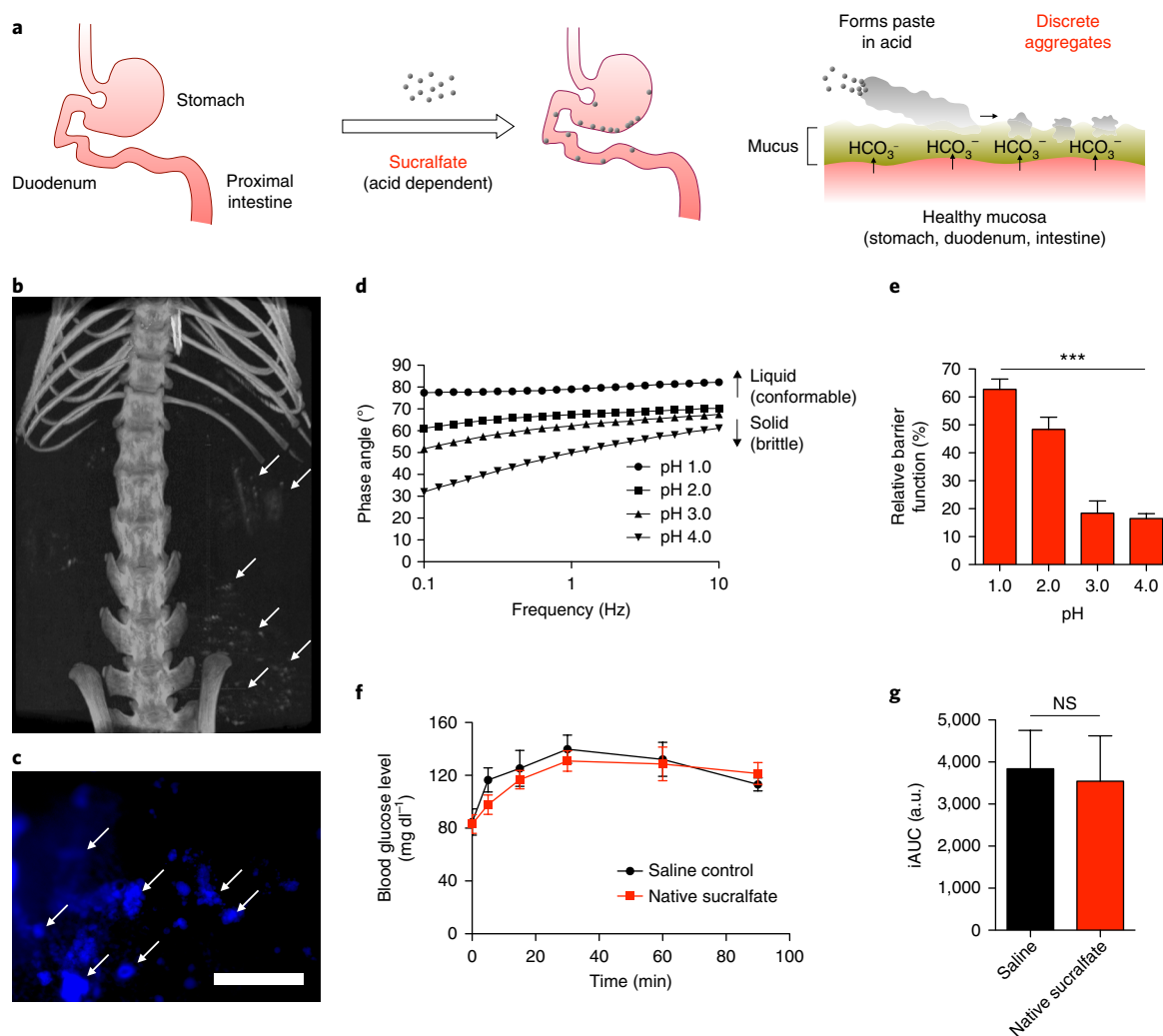


**Fig. 2 | In vivo assessment of the behaviour of sucralfate gavigated into the stomach of healthy non-ulcerative SD rats.** **a**, Due to the pH sensitivity of sucralfate, the sucralfate paste solidifies on healthy mucosa to form brittle and discrete aggregates that are not suitable for a barrier coating. **b**, Representative CT image of SD rat gavigated with sucralfate (1 h time point). A small amount of sucralfate is sparsely scattered in the stomach and lower intestine. Supplementary Movies 1 and 2 give the 3D projection of the full CT scan. **c**, Representative fluorescence microscopy image of a harvested stomach of a sucralfate-gavigated rat (1 h time point). Sucralfate was specifically labelled blue using quinine staining. Scale bar, 500  $\mu\text{m}$ . **d, e**, Change in rheological properties (**d**) and barrier functions (**e**) of acidified sucralfate pastes (reacted in simulated gastric fluid (SGF) (pH 1.0)) in solutions with multiple pHs (1.0–4.0). With an increase in the surrounding pH, acidified sucralfate pastes showed lower phase angles, which indicates that they solidify in a higher pH similar to that in the duodenal environment, and thus the barrier properties are steeply decreased. One-way analysis of variance (ANOVA) ( $n=3$  per arm,  $***P<0.0001$ ). **f, g**, OGTT curves (**f**) and area under curve (**g**) after a  $0.5\text{ g ml}^{-1}$  glucose solution was gavigated into SD rats that were pregavigated with sucralfate 1 h before. No significant difference was observed between the OGTT results of SD rats gavigated with sucralfate or with saline solution. Student *t*-test ( $n=3$  per arm, NS, not significant). a.u., arbitrary units.

a dried formulation that is highly desirable for oral administration (we named the compound LuCI (luminal coating of the intestine)). To synthesize LuCI, the native sucralfate was reacted with HCl solutions in water with concentrations higher than that of stomach acid to break irreversibly the hydroxyl linkages by excessive protonation/hydration to form shorter PAC chains that contain more bound water ( $-\text{OH}_2$ ) (Fig. 3a). In HCl solutions with concentrations higher than about 0.3 N, they formed translucent water-immiscible viscous liquids (that is, paste) (Fig. 3b). The viscosity of the pastes could be controlled with the HCl concentration of the reaction solution. When the HCl concentration was elevated from 0.3 N to 0.6 N, the viscosity of the resultant paste controllably decreased from  $79.84 \pm 9.41$  Pas to  $4.38 \pm 1.72$  Pas (Fig. 3c). We believe this ability to control the viscosity of LuCI could have important implications for the onset of action, the location and extent of the coating,

and the durability of the coating. The number of hydroxy groups and the degree of polymerization of PAC in LuCI was further analysed (via the number of aluminium ions per PAC molecule) using the titration-based method reported previously<sup>16,17</sup>. The number of hydroxy groups per aluminium in LuCI was lower than that of sucralfate and exhibited a linear correlation to the HCl concentration used in the fabrication of LuCI (Fig. 3d). This indicates that the acid-dependent hydroxyl linkages were broken and converted into bound water, which is further supported by thermogravimetric analysis and Fourier transform infrared spectroscopy analysis (Supplementary Fig. 2).

The resultant LuCI pastes could be reversibly dehydrated to prepare dried powder formulations using multiple drying methods, such as lyophilization, microwave and solvent-mediated dehydration (Fig. 3e). When the dried LuCI powders were added

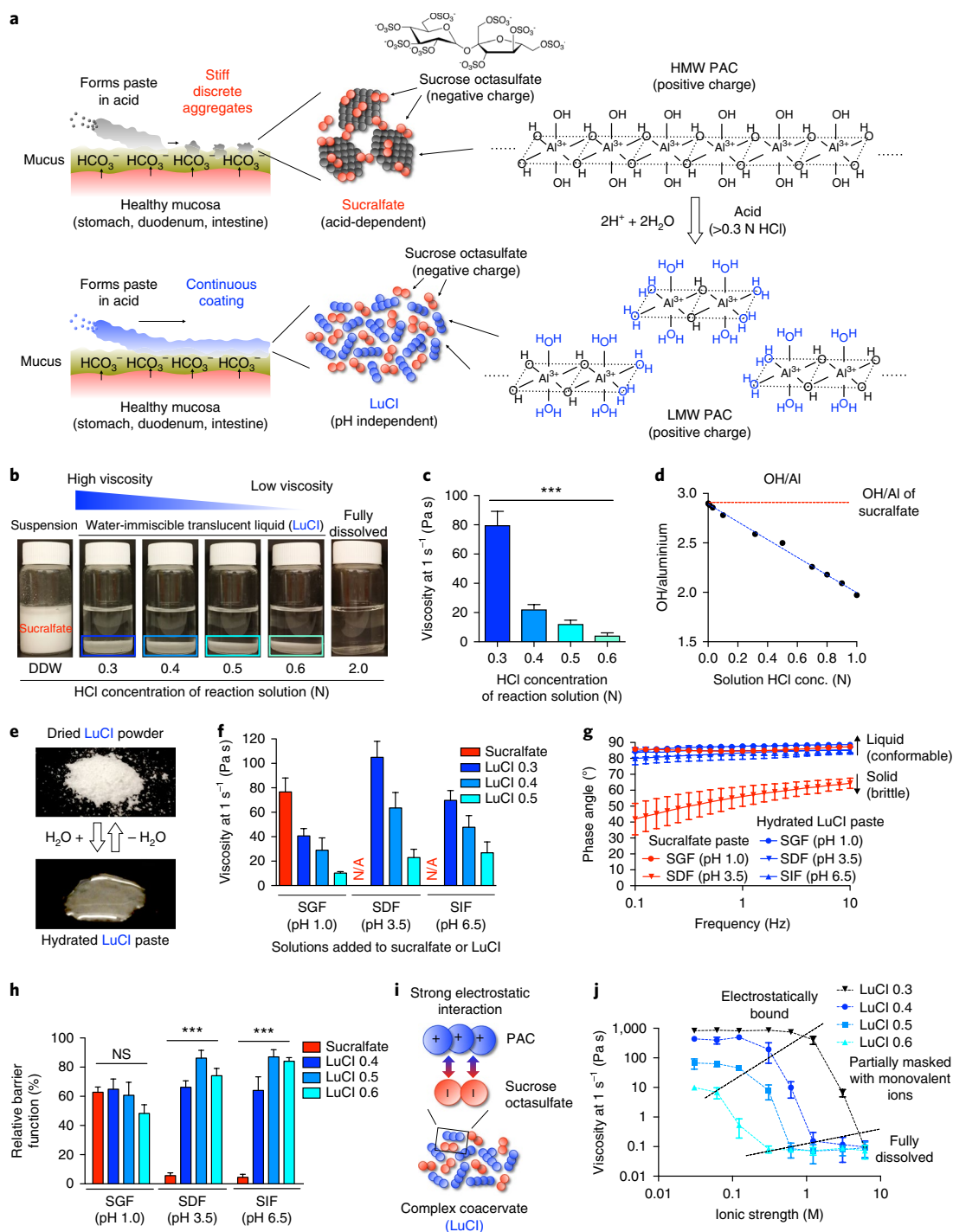


**Fig. 3 | Fabrication and physicochemical properties of LuCl.** **a**, Schematic representations of the physical and chemical structures of sucralfate and LuCl. **b**, Reaction of sucralfate in high-concentration HCl solutions (0.3–0.6 N HCl in water) to form translucent water-immiscible translucent liquids (that is, paste) with different viscosities. **c**, Viscosity of the acidified sucralfate paste reacted in HCl solutions (0.3–0.6 N). The viscosity decreased with a higher concentration of the HCl. One-way ANOVA ( $n=3$  per arm,  $***P<0.0001$ ). **d**, The number of hydroxy groups per number of aluminium (OH/Al) of LuCl fabricated using HCl solutions in different concentrations measured using a titration method. **e**, Reversible dehydration/hydration of LuCl to form a dried powder formulation that quickly forms a sticky paste in an aqueous environment. **f**, Viscosity of sucralfate and dehydrated LuCl in different simulated body fluids, which include simulated gastric fluid (SGF) (pH 1.0), simulated duodenal fluid (SDF) (pH 3.5) and simulated intestinal fluid (SIF) (pH 6.5). N/A, did not form paste. **g**, Change of rheological properties of dried LuCl powder rehydrated in different simulated gastrointestinal fluids. **h**, Relative barrier function of LuCl tested using glucose solutions in different simulated body fluids (120 g l<sup>-1</sup>). One-way ANOVA ( $n=3$  per arm,  $***P<0.0001$ ). **i**, Schematic representation of complex coacervation in LuCl between anionic sucrose octasulfate and cationic LWM PAC. The two polyelectrolytes are bound via a strong electrostatic interaction to form a liquid that is insoluble in water. **j**, Change in viscosity of rehydrated LuCl in NaCl solutions with different ionic strengths. With increasing ionic strength, the viscosity of rehydrated LuCl pastes decreased due to partial masking of the charged groups in PAC and sucrose octasulfate of LuCl, and fully dissolved in NaCl solutions with a high ionic strength. This is a characteristic behaviour of complex coacervate systems. Sucralfate and LuCl fabricated using HCl solutions with concentrations lower than 0.3 N did not dissolve in NaCl solutions.

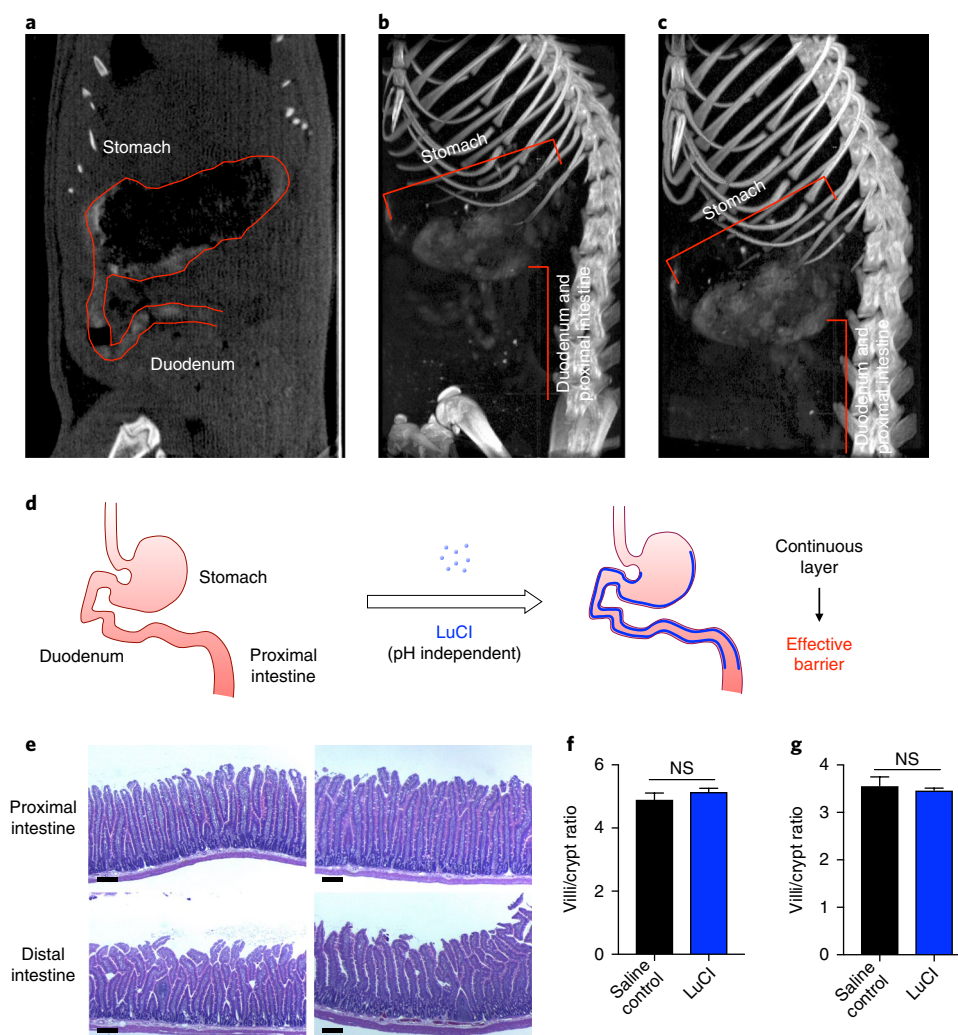


**Fig. 4 | In vivo assessment of the behaviour of LuCI gavigated into the stomach of rats using CT imaging.** **a**, Coronal plane view of SD rats that were gavaged with LuCI 1 h prior to the imaging. LuCI formed a layer in stomach, duodenum and proximal intestine. **b,c**, 3D view of SD rats gavaged with LuCI 1 h (**b**) and 5 h (**c**) before the CT imaging. LuCI attaches to the stomach, duodenum and proximal intestine for at least 5 h after gavage (Supplementary Movies 5–7 show a 3D reconstruction of the full CT scan), whereas sucralfate only formed sparsely scattered aggregates on the healthy mucosa (Fig. 2b,c and Supplementary Movies 1 and 2). **d**, Schematic representation of the luminal barrier coating provided by LuCI through oral administration. **e**, Representative histology images of rat proximal and distal intestines. For the saline control group (left), SD rats were gavaged with the same volume of saline solution (0.9% w/v) ( $n=3$ ) daily for 6 d, and for the LuCI group (right), SD rats were gavaged with LuCI (450 mg per kg rat,  $n=3$ ) daily for 6 d. Scale bar, 50  $\mu\text{m}$ . **f,g**, Average proximal intestine villi/crypt ratio (**f**) and distal intestine villi/crypt ratio (**g**) of each group. Student *t*-test (two-tailed,  $n=3$  per arm).

with water (pH 7.0) or any type of simulated body fluid at different pH levels, they immediately formed water-immiscible liquids with viscosities similar to the pastes formed prior to dehydration. The native sucralfate did not form a viscous paste in water (pH 7.0) and formed a suspension in SDF (pH 3.5) and in SIF (pH 6.5) (Fig. 3f). When the LuCI paste, hydrated in SGF (pH 1.0), was added to pH 3.5 SDF and pH 6.5 SIF, the phase angle of the resultant pastes was higher than  $80^\circ$ , which indicates that the resultant pastes were in a liquid state, whereas the acidified sucralfate paste that was transferred from pH 1.0 SGF to SDF or SIF showed significant decrease in the phase angle or formed weak brittle solid particles (Fig. 3g). This suggests that the LuCI can potentially be hydrated into a conformable coating independent of the location in the gastrointestinal tract, unlike native sucralfate. In addition, the hydration-based system generated significantly less free aluminium compared to the native sucralfate (Supplementary Fig. 3). In SGF, LuCI

blocked 50–60% of the glucose transport, similar to sucralfate, and in higher pH environments using SDF and SIF, LuCI showed an enhanced barrier function (up to ~83% glucose was blocked) compared to sucralfate, which exhibited significantly decreased barrier properties in these conditions (Fig. 3h). These results show that, unlike sucralfate, the barrier property of LuCI is retained in higher pH environments similar to the environment at different locations in the gastrointestinal tract. This barrier function of LuCI is probably due to the complex coacervation between PAC and sucrose octasulfate in which the two oppositely charged polyelectrolytes bind together via a strong electrostatic interaction to form a water-insoluble liquid (Fig. 3i). Sucralfate and LuCI fabricated using HCl solutions with concentrations lower than 0.3 N did not dissolve in the saturated NaCl solution (~6 M) (Supplementary Fig. 4). When LuCI powders were added to NaCl solutions in high concentrations (>0.5 M), they formed less viscous pastes with increasing NaCl concentrations due to a partial

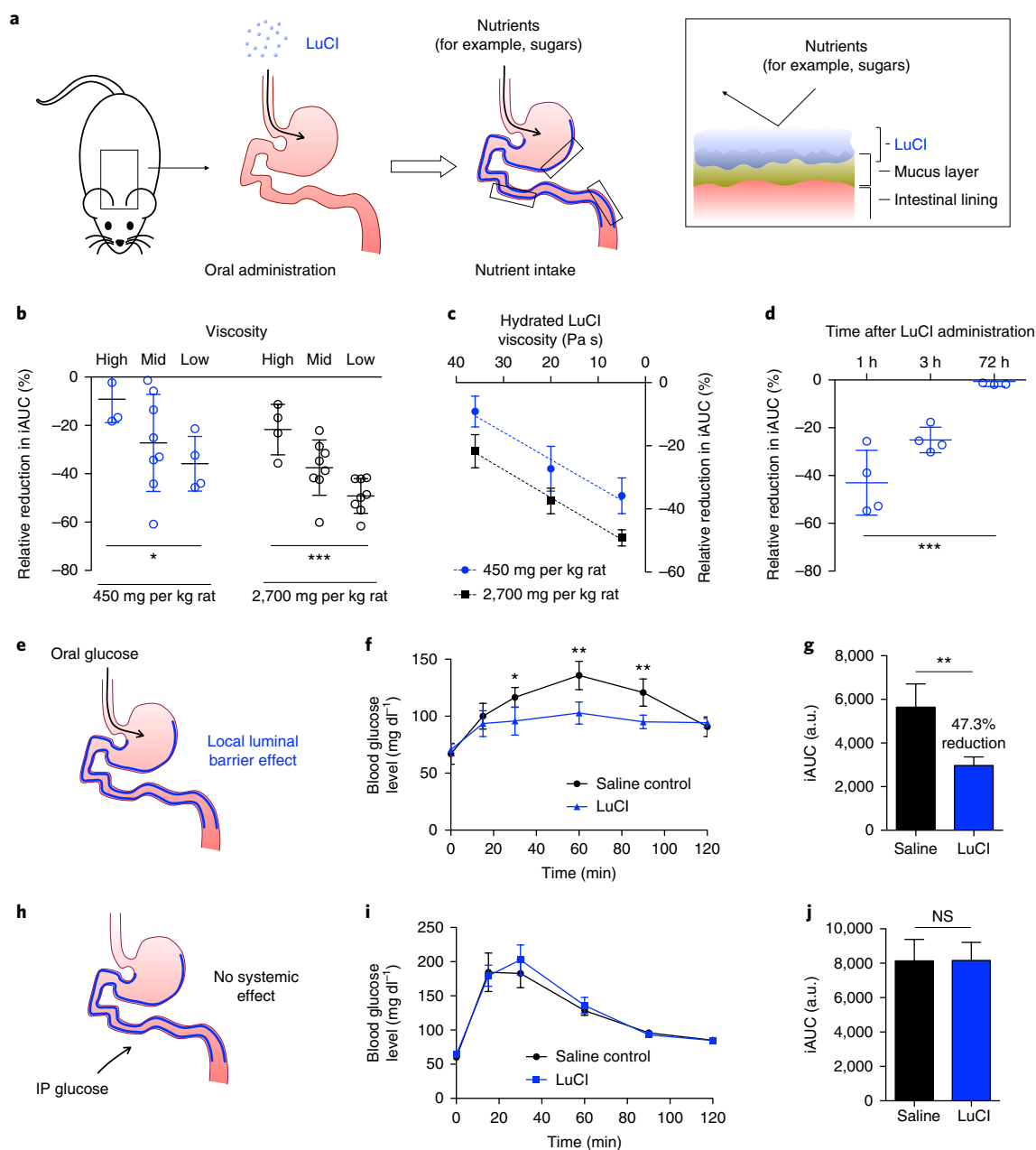


**Fig. 5 | Reduced glucose response with LuCI administration in rats.** LuCI fabricated using 0.4 N, 0.5 N or 0.6 N HCl solutions and rehydrated in 0.9% w/v normal saline is denoted as 'LuCI viscosity high', 'LuCI viscosity mid' and 'LuCI viscosity low', respectively. **a**, Schematic representation of an *in vivo* rat OGTT study for LuCI's barrier function against nutrients (such as sugars). **b**, Reduction of glucose responses in the iAUC of SD rats gavaged with LuCI pastes in different viscosities and doses. One-way ANOVA ( $*P < 0.05$ ,  $***P < 0.0001$ ). **c**, Correlation between the LuCI viscosity in two different doses and iAUC. **d**, Percentage reduction of iAUC in OGTT with different LuCI dosing schedules. One-way ANOVA ( $n = 4$  per arm,  $***P < 0.0001$ ). **e**, Representative schematic of the local barrier effect of LuCI in OGTT with orally administered glucose. **f**, OGTT curves of rats gavaged with LuCI pastes. Rats gavaged with 0.9% w/v normal saline were used as a control in place of LuCI. Student *t*-test (two-tailed,  $n = 4$  per arm,  $*P < 0.05$ ,  $***P < 0.001$ ). **g**, iAUC of the OGTT curves in **f**. Student *t*-test (two-tailed,  $n = 4$  per arm,  $**P < 0.001$ ). **h**, Representative schematic of the no systemic effect of LuCI in IPGTT with systemically IP-administered glucose. **i**, IPGTT curves of rats gavaged with LuCI pastes. Rats gavaged with 0.9% w/v normal saline were used as the control. Student *t*-test (two-tailed,  $n = 4$  per arm). **j**, iAUC of the OGTT curves in **i**. Student *t*-test (two-tailed,  $n = 4$  per arm).

masking of the charged polymers with monovalent ions, and fully dissolved in higher NaCl concentrations above a critical level (Fig. 3j). In addition, the LuCI paste showed no swelling in SGF (pH 1.0) and SIF (pH 6.5) for two hours (Supplementary Fig. 5). These results are characteristic complex coacervate behaviours<sup>18–20</sup> that support LuCI as being an excellent candidate for intestine coating compared to other gelatinous materials.

We assessed LuCI's ability to form a coating on the gastrointestinal tract. In a preliminary *ex vivo* test, LuCI hydrated in SIF was manually spread on a freshly harvested small intestine mucosa and it rapidly attached onto the mucosa to form a translucent layer (Supplementary Movie 3) that remained strongly attached in normal saline solution (0.9% w/v) even with vigorous shaking (Supplementary Movie 4). To further assess LuCI's ability to

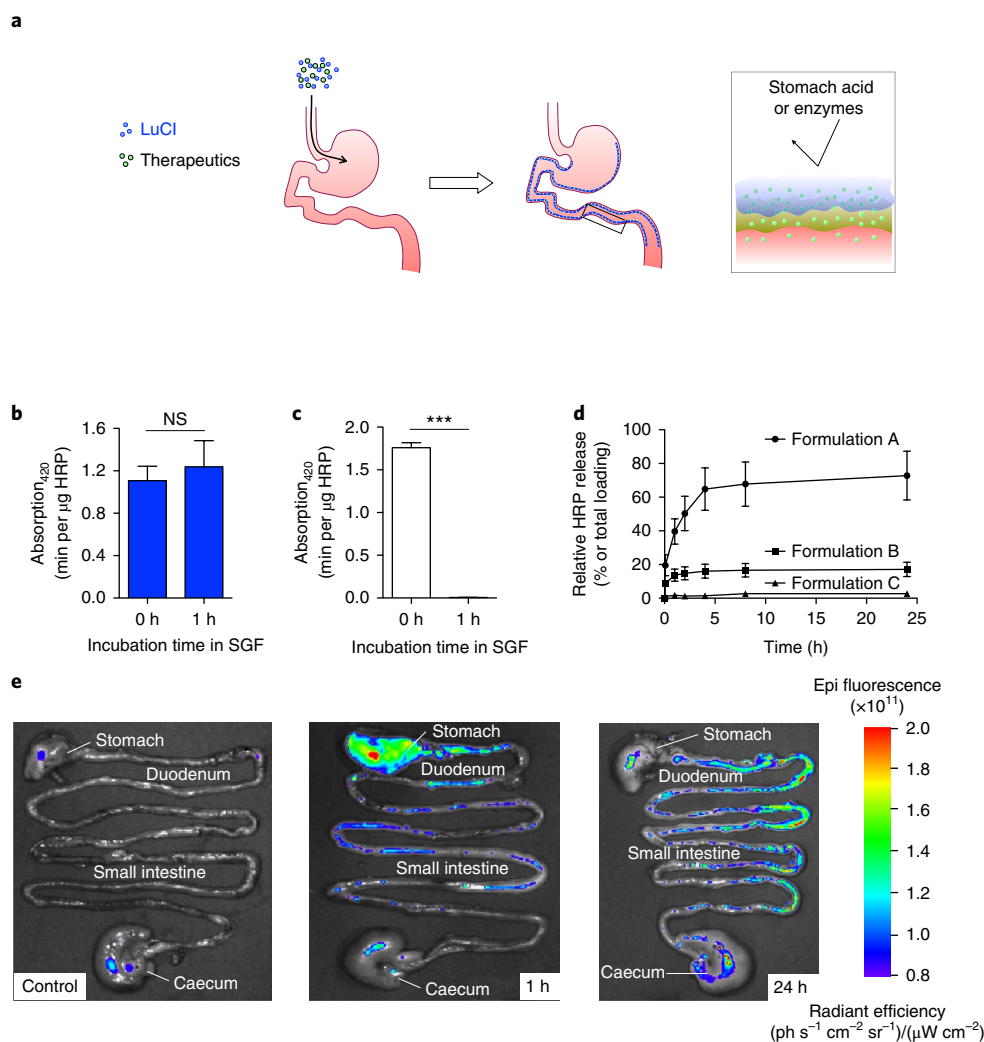


**Fig. 6 | Delivery of protein using LuCI on the proximal intestine.** **a**, The illustration shows oral administration and mucoadhesive drug delivery using LuCI. **b**, HRP activity in LuCI before and after a 1 h treatment in a SGF (pH 1.0) normalized by the remaining amount of HRP activity. Student *t*-test (two-tailed). **c**, Naked HRP activity (without a carrier) before and after 1 h of incubation in a SGF (pH 1.0). Student *t*-test (two-tailed,  $***P < 0.0001$ ). **d**, The release of HRP from LuCI using different formulations. Formulation A, dry LuCI powder mixed in dry HRP powder; Formulation B, dry LuCI powder + HRP solution in PBS (pH 7.4); Formulation C, hydrated LuCI paste in PBS (pH 7.4) + HRP solution in PBS (pH 7.4). **e**, Fluorescence image analysis using IVIS to track the fluorescence-tagged model protein (FITC-albumin) encapsulated in LuCI. Rats were gavaged with LuCI (450 mg per kg rat) loaded with FITC-bovine serum albumin (BSA) (2% w/w in LuCI powder), and the gastrointestinal tracts from stomach to caecum were harvested after 1 h or 24 h for fluorescent imaging using an IVIS in vivo imaging system. Rats without LuCI gavage were used as the control. Compared to the total fluorescence found,  $46.8 \pm 24.1\%$  fluorescence was retained in the gut after 1 h. ph, photons.

form a coating in vivo, SD rats were gavaged with hydrated LuCI pastes followed by CT imaging (details are given in Supplementary Fig. 6). The CT images taken within one hour of gavage showed that the LuCI pastes formed a layer in the stomach, duodenum and small intestine, and the layer was stable for the extent of the study (five hours) (Fig. 4a–c and Supplementary Movies 5 and 6). After 24 hours, a scattered LuCI signal was found in the lower gastrointestinal tract (Supplementary Fig. 7 and Supplementary Movie 7), which indicates that the LuCI coating is transient. These data collectively suggest that the LuCI can form a coating on the luminal side of the gastrointestinal tract with transient stability (Fig. 4d). To further assess the biocompatibility of LuCI, SD rats were gavaged with LuCI daily ( $n=3$ , 450 mg per kg rat) for six days and their gastrointestinal tracts were harvested for histological assessments. The epithelial layers of both the proximal and distal bowels were intact and appeared similar to those of the saline control group rats

gavaged with saline solution (0.9% w/v,  $n=3$ ) (Fig. 4e). Villi/crypt ratios (that is, the ratio between villi length and crypt depth) of both proximal and distal bowels were unchanged (Fig. 4f,g) and the rats did not develop diarrhoea and did not show weight loss during the study, which suggests a favourable biocompatibility of LuCI on the gastrointestinal mucosa (Supplementary Fig. 8).

We then assessed if the LuCI coating could act as a nutrient barrier and, importantly, lower glucose response after an oral glucose load using a standard OGTT (Fig. 5a). We hypothesized that the continuous LuCI coating on the gastrointestinal mucosa could significantly lower the glucose response and further hypothesized that the control of the viscosity of LuCI paste can maximize the barrier function by altering the thickness and area of the barrier coating. The viscosity of the LuCI paste had a significant impact on the reduction of the blood glucose response (Fig. 5b,c). The LuCI formulation that formed a lower viscosity pastes (viscosity, 5 Pa s, a  $35.8 \pm 11.3\%$

reduction in iAUC compared to the normal saline control) exhibited a significantly higher reduction of blood glucose responses compared to higher viscosity pastes (viscosity, 36 Pas,  $9.1 \pm 9.7\%$  reduction in iAUC). The higher viscosity paste exhibited a similar viscosity with the paste formed from native sucralfate via a reaction with SGF. The duration between the LuCI administration and glucose gavage also affected the reduction of blood glucose depending on the administered LuCI formulation (Fig. 5d). One hour after the low viscosity LuCI treatment, the reduction in the glucose response was  $43.0 \pm 13.6\%$ , and three hours after treatment, the reduction decreased to  $25.1 \pm 5.4\%$ . This reduction in glucose response was completely reversed after three days ( $0.7 \pm 2.1\%$  reduction) and the OGTT curves were similar to those of the control group gavaged with 0.9% w/v saline solution without LuCI. These results suggest that the oral administration of LuCI can effectively lower the glucose response by forming a transient and reversible barrier to glucose, and the reduction in glucose responses can be maximized by altering the physical properties of LuCI (for example, viscosity) that probably modulate the duration and location of the coating. We further hypothesized that the LuCI coating has an effect on the glucose response through acting as a local physical barrier and not through a systemic effect. We compared the impact of LuCI treatment on an OGTT to an intraperitoneal (IP) injection (for IP glucose tolerance tests (IPGTTs)). Although an OGTT assesses the impact that LuCI has on glucose absorption, the IPGTT bypasses the step of intestinal absorption by delivering the glucose to the gastrointestinal tract without a physical barrier, and tests for a possible systemic effect of LuCI through hepatic or other effects. In OGTT (Fig. 5e), the blood glucose responses were significantly reduced (Fig. 5f), whereas iAUC was reduced by  $47.3 \pm 7.0\%$  (Fig. 5g). However, for IPGTT (Fig. 5h), there was no difference in the glucose response in IPGTT curves (Fig. 5i) and in iAUC (Fig. 5j), which suggests that LuCI's mechanism of a reduced glucose response is due to a localized barrier coating of the intestine and not to a systemic effect.

We showed that LuCI forms a transient physical barrier on the luminal surface of the gastrointestinal tract and, in essence, emulates a critical part of bariatric surgery in a non-invasive way. Recently, bariatric surgery has been shown in multiple randomized clinical trials to be superior to traditional pharmaceuticals in managing T2D<sup>2,5,21,22</sup>. In fact, 80% of the patients who have RYGB experience early remission of their T2D. However, the risks of surgery along with permanent changes to the gastrointestinal anatomy have hampered widespread acceptance. As a result, the majority of patients, who include non-obese patients with T2D and patients who are highly susceptible to develop T2D (for example, prediabetic) are not eligible for the surgeries, and even among those who are eligible (patients who have a body mass index over  $40 \text{ kg m}^{-2}$ ), less than 1–2% actually undergo the procedure. As a less-invasive alternative, the duodenojejunal endoscopic sleeve was developed to prevent contact between food and the duodenal mucosa, and showed promising results in remitting T2D in patients, which validates the concept that isolation of the proximal bowel from nutrient exposure can lead to dramatic improvements in T2D<sup>23,24</sup>. In clinical studies with T2D patients, the isolation of the proximal gut was shown to induce weight loss and to improve metabolic parameters, which include glucose homeostasis (for example, glucose responses and HbA1c) and insulin sensitivity (for example, homeostatic model assessment indices)<sup>23–25</sup>. However, the sleeve is implanted endoscopically, requires annual device removal and its pivotal FDA trial was recently halted due to serious complications. There is thus an urgent need for a safe, non-invasive and effective treatment with broad applicability for diabetic patients. We expect that LuCI, an orally administered intestine barrier coating that can transiently reduce the postprandial glucose response, could be a therapeutic approach that is safer and associated with significantly less complications, and thus can potentially help a wide T2D patient population.

We further explored the ability of LuCI to deliver biologics. Given LuCI's physical state as a paste, it was expected that biologics (for example, proteins) could be delivered in LuCI to reach the proximal intestine without succumbing to the harsh environmental factors, such as stomach acid and other intestinal fluids (Fig. 6a). To demonstrate LuCI's ability to protect loaded proteins from stomach acid, a model protein horseradish peroxidase (HRP) was loaded in LuCI and exposed to SGF (pH 1.0) for one hour. The HRP that remained loaded in the LuCI showed a similar activity before and after the acid treatment (Fig. 6b), whereas naked HRP exposed to the acid showed a complete loss of activity (Fig. 6c). The loaded HRP could be released from LuCI and the release rate could be tuned by modifying the method of formulation (Fig. 6d). When dry HRP powder was directly mixed with dry LuCI powder (loading, 2% w/w in LuCI; loading efficiency, 84%), ~62% of the loaded HRP was gradually released from the LuCI during the first four hours and an additional ~10% of the HRP was released over the course of 24 hours. When the dry-mixture formulation of LuCI loaded with a fluorescent-tagged model protein (fluorescein isothiocyanate (FITC)–albumin) was gavaged to rats, the protein cargo could be delivered to duodenum and small intestine (Fig. 6e). The fluorescence signal from the model protein was detected mostly in the stomach and duodenum after one hour, and on the duodenum and small intestine even after 24 hours when the earlier CT images showed no remaining LuCI (Supplementary Fig. 9), which indicates that the model protein was probably released and retained on the gut. Thus, in addition to modulating nutrient absorption, LuCI may find clinical use as a protein delivery vehicle.

## Methods

Methods, including statements of data availability and any associated accession codes and references, are available at <https://doi.org/10.1038/s41563-018-0106-5>.

Received: 1 May 2017; Accepted: 10 May 2018;  
Published online: 11 June 2018

## References

- American Diabetes Association 2 Classification and diagnosis of diabetes. *Diabetes Care* **39** S13–S22; erratum. *Diabetes Care* **39**, 1653 (2016).
- Mingrone, G. et al. Bariatric surgery versus conventional medical therapy for type 2 diabetes. *N. Engl. J. Med.* **366**, 1577–1585 (2012).
- Lovshin, J. A. & Drucker, D. J. Incretin-based therapies for type 2 diabetes mellitus. *Nat. Rev. Endocrinol.* **5**, 262–269 (2009).
- Drucker, D. J. & Nauck, M. A. The incretin system: glucagon-like peptide-1 receptor agonists and dipeptidyl peptidase-4 inhibitors in type 2 diabetes. *Lancet* **368**, 1696–1705 (2006).
- Stefater, M. A., Wilson-Pérez, H. E., Chambers, A. P., Sandoval, D. A. & Seeley, R. J. All bariatric surgeries are not created equal: insights from mechanistic comparisons. *Endocr. Rev.* **33**, 595–622 (2012).
- Rubino, F. et al. The early effect of the Roux-en-Y gastric bypass on hormones involved in body weight regulation and glucose metabolism. *Ann. Surg.* **240**, 236–242 (2004).
- Jorgensen, N. B. et al. Acute and long-term effects of Roux-en-Y gastric bypass on glucose metabolism in subjects with Type 2 diabetes and normal glucose tolerance. *Am. J. Physiol. Endocrinol. Metab.* **303**, E122–E131 (2012).
- Zhang, S., Bellinger, A. M., Glettig, D. L. & Barman, R. A pH-responsive supramolecular polymer gel as an enteric elastomer for use in gastric devices. *Nat. Mater.* **14**, 1065–1073 (2015).
- Zelikin, A. N., Ehrhardt, C. & Healy, A. M. Materials and methods for delivery of biological drugs. *Nat. Chem.* **8**, 997–1007 (2016).
- Fuhrmann, G. Sustained gastrointestinal activity of dendronized polymer-enzyme conjugates. *Nat. Chem.* **5**, 582–589 (2013).
- Danesh, B. J., Duncan, A. & Russell, R. I. Is an acid pH medium required for the protective effect of sucralfate against mucosal injury? *Am. J. Med.* **83**, 11–13 (1987).
- Morris, G. P. (eds D. Hollander & G. Tytgat) *Sucralfate: From Basic Science to the Bedside*. 71–82 (Springer, New York, NY, 1995).
- Nagashima, R. Mechanisms of action of sucralfate. *J. Clin. Gastroenterol.* **3**, 117–127 (1981).
- Ochi, K. (eds D. Hollander & G. Tytgat) *Sucralfate: From Basic Science to the Bedside*. 47–58 (Springer, New York, NY, 1995).

15. McCarthy, D. M. Drug therapy: sucralfate. *New Engl. J. Med.* **325**, 1017–1025 (1991).
16. Nail, S. L., White, J. L. & Hem, S. L. Structure of aluminum hydroxide gel. I: Initial precipitate. *J. Pharm. Sci.* **65**, 1188–1191 (1976).
17. Hem, J. D. & Roberson, C. E. *Form and Stability of Aluminum Hydroxide Complexes in Dilute Solution* Water Supply Paper 1827-A (Geological Survey, Washington DC, 1967).
18. Wang, Q. & Schlenoff, J. B. The polyelectrolyte complex/coacervate continuum. *Macromolecules* **47**, 3108–3116 (2014).
19. de Kruif, C. G., Weinbreck, F. & de Vries, R. Complex coacervation of proteins and anionic polysaccharides. *Curr. Opin. Colloid Interface Sci.* **9**, 340–349 (2004).
20. Veis, A. & Aranyi, C. Phase separation in polyelectrolyte systems. I. Complex coacervates of gelatin. *J. Phys. Chem.* **64**, 1203–1210 (1960).
21. Cummings, D. E. & Flum, D. R. Gastrointestinal surgery as a treatment for diabetes. *J. Am. Med. Assoc.* **299**, 341–343 (2008).
22. Couzin, J. Bypassing medicine to treat diabetes. *Science* **320**, 438–440 (2008).
23. Betzel, B. et al. Weight reduction and improvement in diabetes by the duodenal–jejunal bypass liner: a 198 patient cohort study. *Surg. Endosc.* **31**, 2881–2891 (2016).
24. Koehestanie, P. et al. Duodenal–jejunal bypass liner implantation provokes rapid weight loss and improved glycemic control, accompanied by elevated fasting ghrelin levels. *Endosc. Int. Open* **2**, E21–E27 (2014).
25. Cohen, R. et al. Role of proximal gut exclusion from food on glucose homeostasis in patients with Type 2 diabetes. *Diabetes Med.* **30**, 1482–1486 (2013).

## Acknowledgements

This work was supported by NIH grant GM086433 to J.M.K., NIH grant DK084064 to A.T., Partners Innovation Development Grants Program and BRI Translational Technologies and Care Innovation Grant from Brigham Research Institute (BRI) to

J.M.K. and A.T., Diabetes Action Research and Education Foundation Grant to J.M.K., Accelerator Award from CIMIT to J.M.K. and A.T., the Basic Science Research Program through the National Research Foundation of Korea (NRF) funded by the Ministry of Education of Korea (2012R1A6A3A03041166) and the Korea Institute for Advancement of Technology (N0002123) to Y.L. This work was supported in part by the Netherland–America Foundation (NAF) Fulbright Fellowship, the Ivy Circle Award and the Prince Bernard Culture Foundation Award to T.E.D. We thank J.N.M. IJzermans at Erasmus University Medical Center, Rotterdam, for his role as educational supervisor to T.E.D. The authors thank J. Tolkoff and F. Schoen for critical feedback. We thank S. Wang for the CT imaging and W. Li for the IVIS imaging.

## Author contributions

Y.L., T.E.D., A.T. and J.M.K. developed the concept and designed experiments. Y.L., T.E.D., K.C. and D.S.Y.L. conducted the experiments. Y.L., T.E.D., K.C., D.S.Y.L., A.T. and J.M.K. analysed the data. Y.L., T.E.D., A.T. and J.M.K. wrote the manuscript. All the authors provided critical comments on the manuscript.

## Competing interests

The authors declare no competing interests.

## Additional information

**Supplementary information** is available for this paper at <https://doi.org/10.1038/s41563-018-0106-5>.

**Reprints and permissions information** is available at [www.nature.com/reprints](http://www.nature.com/reprints).

**Correspondence and requests for materials** should be addressed to Y.L. or A.T. or J.M.K.

**Publisher's note:** Springer Nature remains neutral with regard to jurisdictional claims in published maps and institutional affiliations.

## Methods

**Integrative barrier property test using mucin-coated membrane.** To examine barrier properties *in vitro*, a mucin-coated membrane was prepared to mimic the mucus surface of the intestine (Fig. 1b). Given that the mucoadhesion of a material mostly depends on the interfacial interaction between the mucin and material, a layer of mucin was attached to a porous membrane to mimic the surface of the unstirred layer of mucus. In addition, given the inhomogeneity of mucus from different animal sources and ethical issues (that is, animal sacrifice), extracted and purified mucin with a fixed concentration was used to achieve reproducible results throughout the screening of multiple candidate materials. Specifically, a cellulose nitrate membrane (pore size 0.45  $\mu\text{m}$  (Whatman)) was incubated in a 3% w/v porcine stomach mucin (Sigma-Aldrich) solution in PBS (pH 7.4) and gently shaken for 2 h at room temperature. The membrane was washed with distilled deionized water (DDW, pH 5.5) to remove the excess mucin solution. The mucin-coated membranes were used within 1 h of preparation. To measure the thickness of the mucin layer, the mucin-coated membrane was lyophilized and imaged using a scanning electron microscope and the thickness of randomly selected positions was examined (average mucin layer thickness,  $\sim 100\ \mu\text{m}$ ).

To test the nutrient barrier properties, 1 ml of a 1 w/v% candidate polymer solution in a simulated stomach acid (pH 1.0) was first applied evenly to a mucin-coated membrane and vertically tilted for 1 min. Exceptions to this procedure using DDW (pH 7) instead of the simulated stomach acid were imposed for alginate, nanocellulose (Supplementary Information) and chitosan/heparin nanoparticles (Supplementary Information). To determine the coating efficiency of each material, the material-attached membrane was lyophilized after predetermined incubation times in the simulated stomach acid (pH 1.0) (5 min; 10, 15 and 20 min for selected materials) followed by dry weight analysis. The dry weight was calculated from dry weights of material-attached membranes and mucin-coated membranes. The material attached to the mucin-coated membrane was mounted in a Franz-cell system, 3 ml of glucose solution ( $120\ \text{g l}^{-1}$ ) was added and the samples were collected from the receiver part of the system after 5 min (10, 15 and 20 min for selected materials; up to 3 h for sucralfate). The permeation tests were performed in triplicate for each material. The glucose concentration was measured using high performance liquid chromatography (HPLC) (Agilent) with an analytical C18 column (Zorbax Eclipse XDB-C18 (Agilent)). The flow rate was  $1\ \text{ml min}^{-1}$ , the eluent was DDW and the wavelength of the ultraviolet detector was 195 nm. All the results were normalized to a mucin-coated membrane without the application of a test material (0% blocked).

**Rheological measurements.** Rheological properties were analysed using a rheometer (AR-G2 (TA Instruments)). The dynamic viscosity of each material solution was measured using a 20 mm plate with 200  $\mu\text{m}$  gaps (shear rate,  $0.01\text{--}100\ \text{s}^{-1}$  in log scale; a shear rate of  $1\ \text{s}^{-1}$  was selected to compare viscosity of materials). The dynamic phase angle was measured using a frequency sweep (frequency range, 0.1–10 Hz in log scale).

**Fabrication of dried LuCI particles using a solvent dehydration method and a microwave-assisted dehydration method.** In the solvent-based dehydration, the acidified sucralfate paste was added with an excess amount of water-miscible common solvents (for example, ethanol, methanol, dimethylsulfoxide (DMSO) and acetone), and stirred to form a suspension in a brittle particle form that was further dried in vacuum to evaporate the solvents. Briefly, to fabricate the dry particles using solvent-based dehydration, sucralfate was first treated with acid (0.3–0.8 N HCl solutions) to form a viscous sticky paste that was further combined with water-soluble solvents (for example, alcohol, acetone, DMSO and dimethylformamide) and vortexed, which resulted in a white particle suspension. The suspension was then dried to remove the solvent and the dried particles were further ground to form a white powder. In the microwave-assisted dehydration, the acidified sucralfate paste was placed in a microwave oven, exposed to a 1,200 W microwave for 30 s and ground into a white powder using a mortar and pestle. To gavage LuCI into the rat stomach, the dried powder was hydrated in normal saline solution (0.9% w/v) and the resultant paste was gavaged using a gavage needle (bore size, 0.5 mm).

**Degree of polymerization of PACs in sucralfate and LuCI.** The degree of polymerization of PACs in LuCI and the sucralfate molecule was determined using a titration method based on the reversible protonation of hydroxyl linkages in the PAC backbone<sup>27</sup>. Approximately 10 mg of LuCI was treated with 0.1–0.5 N HCl solutions in different tubes. The samples were vortexed for 5 s followed by 1 h of incubation. The supernatant of each sample was then collected, and the pH was measured using a pH meter. The same procedures were performed with sucralfate. The pH of the HCl solutions was also measured to calculate the difference between the control and the LuCI groups. The difference in pH corresponds to the proton consumption and the amount of hydroxyl linkages, which was then used to calculate the number of aluminium atoms per molecule.

**Animals.** All the experimental animal protocols were approved by the Brigham and Women's Hospital Institutional Animal Care and Use Committee. All the animals received humane care in accordance with the 1996 *Guide for the Care and*

*Use of Laboratory Animals* recommended by the US National Institutes (NIH) of Health. Male Sprague-Dawley rats (Harlan) were acclimatized under a 12:12 light:dark cycle (lights on at 7 a.m.) for at least 1 wk with ad libitum access to standard rat chow. Experiments were performed after an overnight fast with access to water.

**CT imaging of rats gavaged with LuCI or sucralfate.** CT imaging was used to visualize the LuCI (or sucralfate) in the gastrointestinal tract in rats. Briefly, the rats were gavaged with the hydrated LuCI pastes (or a sucralfate suspension in 0.9% w/v normal saline) (dose, 450 mg per kg rat). After predetermined time points (for example, 1, 5 or 24 h), the rats were anaesthetized using 3% isoflurane for 1 min and placed in CT with continuous anaesthesia using 1% isoflurane throughout the imaging session. The CT imaging parameters were: current, 150  $\mu\text{A}$ ; voltage, 40 kV; number of projections, 360; shots, four (total imaging time, 7 min). The raw images were processed, restructured into different view axes (including three-dimensional (3D) projections and 3D videos) and analysed using ImageJ (v1.48 (NIH)).

**Histological analysis of the intestine of rats gavaged with LuCI.** To assess the impact of LuCI on epithelium, SD rats were gavaged with LuCI daily for 6 d and their gastrointestinal tracts were harvested for histological assessments. Briefly, rats were fasted overnight before the first gavage day and gavaged with LuCI ( $n = 3$ , 450 mg per kg rat) or 0.9% w/v saline solution ( $n = 3$ ). The rats were fed with a normal diet and water ad libitum after the first gavage. From day 2 to day 6, the rats were gavaged daily with LuCI or saline without fasting. On day 7, the gastrointestinal tracts were harvested, processed for histological assessments and stained using haematoxylin and eosin staining.

**OGTTs and IPGTTs.** To evaluate the *in vivo* effect of LuCI and sucralfate on the postprandial glucose absorption or systemic absorption, SD rats were pregavaged with the hydrated LuCI pastes and subsequently had an OGTT or IPGTT. Given the technical difficulties in gavaging the dry powder (that is, animal discomfort and precise dosing), LuCI was hydrated with a 0.9% w/v saline solution immediately before the gavage. When the dry LuCI was hydrated as a 0.9% w/v saline solution, the 450 mg per kg rat dose for 400–500 g rats (that is, a 180–225 mg dose per rat) results in a paste volume of 0.7–0.9 ml. For the higher 2,700 mg per kg dose, the paste volume was 4.2–5.4 ml. This dosing volume is in accordance with US Department of Agriculture guidelines, which allows up to 16 ml ( $10\text{--}20\ \text{ml kg}^{-1}$ ) for a 400 g rat. In standard OGTT experiments, SD rats were fasted overnight (starting time 7 p.m. the day prior with access to water, duration of fast 15 h prior to treatment with LuCI) and gavaged with sucralfate, LuCI (dose, 450 mg per kg rat) or saline in predetermined dosing schedule. For the high dose (Fig. 5b,c), a LuCI dose of 2,700 mg per kg rat (six times higher than the initial dose) was gavaged. Using the calculation based on body surface area recommended by the FDA, the human-equivalent dose of a 450 mg per kg rat dose is a 72.9 mg per kg human dose. If we consider a 60 kg human, the dosage is  $\sim 4.4\ \text{g}$ , which is less than the recommended maximum daily dose of the raw material sucralfate, and will probably be further reduced through optimization, which includes more-targeted approaches to the coat-specific regions that are most effective in the glucose response reduction. Then, a 0.5 g per ml glucose solution at a dose of 2 g per kg rat was gavaged 1 h after the last gavage to measure changes in glucose levels for 120 min ( $n = 4$  at least per arm). Blood was collected from the tail vein to measure the blood glucose level using a glucometer (OneTouch UltraSmart (LifeScan Inc.)). All the rats received both the saline and LuCI treatment, but on different days. Each data point was plotted with time as the x axis and iAUC was calculated based on the plot and the pregavage glucose level as a baseline. Statistical significance was determined using one-way analysis of variance (ANOVA). Results were considered significant when  $P \leq 0.05$ . In standard IPGTT experiments, SD rats were treated the same as in the OGTT experiments except that the glucose solution (2 g per kg rat) was injected into the peritoneum 1 h after the last gavage of saline, or LuCI, to measure the changes in glucose level for 120 min ( $n = 4$  at least per arm).

**HRP activity and release tests from LuCI.** The HRP-specific substrate 3,3',5,5'-tetramethylbenzidine (TMB) was used to measure the activity of HRP encapsulated in LuCI before and after the acid treatment. Dry HRP powder (1 mg) was homogeneously mixed with 2 g of dry LuCI powder and hydrated using Hank's balanced salt solution (HBSS). HRP-loaded LuCI (20  $\mu\text{l}$ ) was transferred to a 96-well plate (total amount of HRP, 8  $\mu\text{g}$ , calculated using the hydrated volume per dry weight of LuCI). SSF (50  $\mu\text{l}$ , pH 1.0) was added to HRP-loaded LuCI and incubated at 37 °C for 1 h. The SSF was removed and the LuCI paste washed three times with HBSS. The TMB substrate (liquid substrate, supersensitive for ELISA (Sigma-Aldrich)) was used to test the activity of HRP following the manufacturer's manual. Briefly, 50  $\mu\text{l}$  of TMB substrate was added to the LuCI, incubated for 5 min in a shaking incubator (37 °C) and the reaction was stopped using 50  $\mu\text{l}$  of 2.0 N HCl solution in water that also fully dissolved LuCI. The colour change of the resultant solution was measured in a plate reader using a wavelength of 420 nm. HBSS, HRP solution or LuCI without HRP loading were used as the controls. Micro-BCA (mBCA) was used to measure the amount of HRP that remained in LuCI before and after the SSF treatment.

For the release study, 1 mg of dry HRP powder was homogeneously mixed with 50 mg of LuCI (Formulation A, target loading 2% w/w) in a 2 ml Eppendorf tube and hydrated using 1 ml of PBS (pH 7.4). The supernatant was removed and washed three times with PBS. To calculate the loading efficiency, HRP concentration in the supernatant and each washing buffer was measured using mBCA (loading efficiency, ~84%). The washed LuCI was combined with 1 ml of PBS and incubated in a shaking incubator (37 °C) for predetermined time points. The release buffer was collected and replaced with 1 ml of PBS. The time points were 5 min, 30 min, 1 h, 2 h, 4 h, 8 h and 24 h. The HRP concentration of each release buffer was measured using mBCA. In a different formulation (Formulation B), HRP solution (1 mg of HRP in 1 ml of PBS) was added to hydrated LuCI (dry weight, 50 mg), vortexed for 1 min and washed with PBS three times (loading efficiency, ~80%). In another formulation (Formulation C), HRP solution (1 mg of HRP in 1 ml of PBS) was added to dry LuCI powder (50 mg), vortexed for 1 min and washed with PBS three times (loading efficiency, ~99%). The HRP releases of Formulations B and C were tested using the same method and time points described above.

**Fluorescence imaging of harvested rat gastrointestinal tract with LuCI gavage.** SD rats were gavaged with LuCI (dose, 450 mg per kg rat) encapsulated with

FITC-BSA (2% w/w in LuCI powder), and the gastrointestinal tracts from stomach to caecum were harvested after 1 h or 24 h. The harvested gastrointestinal tracts were imaged using an IVIS Spectrum In Vivo Imaging System (Perkin Elmer). Rats without the LuCI gavage were used as the control and all the images were normalized using the control.

**Statistical analysis.** All values in the present study are expressed as mean  $\pm$  s.d. Statistical analysis was performed using GraphPad Prism. The significance between two groups was analysed by a two-tailed Student *t*-test. Sample variance was tested using the *F* test. For multiple comparisons, a one-way ANOVA test was used. In all cases, a *P* value of less than 0.05 was considered significant. Details for statistical analyses for each comparison are reported in Supplementary Table 1.

**Reporting summary.** Further information on experimental design is available in the Nature Research Reporting Summary linked to this article.

**Data availability.** All relevant data are available from the authors, and/or are included within the manuscript and Supplementary Information.

## Life Sciences Reporting Summary

Nature Research wishes to improve the reproducibility of the work that we publish. This form is intended for publication with all accepted life science papers and provides structure for consistency and transparency in reporting. Every life science submission will use this form; some list items might not apply to an individual manuscript, but all fields must be completed for clarity.

For further information on the points included in this form, see [Reporting Life Sciences Research](#). For further information on Nature Research policies, including our [data availability policy](#), see [Authors & Referees](#) and the [Editorial Policy Checklist](#).

Please do not complete any field with "not applicable" or n/a. Refer to the help text for what text to use if an item is not relevant to your study. [For final submission](#): please carefully check your responses for accuracy; you will not be able to make changes later.

### ▶ Experimental design

#### 1. Sample size

Describe how sample size was determined.

The power calculation (oral glucose tolerance test) distinguished as significant a difference of 40% in the outcome variable between test and control group; 15% estimated standard deviation;  $p = 0.05$ ; 90% confidence;  $n = 4$ .

#### 2. Data exclusions

Describe any data exclusions.

N/A

#### 3. Replication

Describe the measures taken to verify the reproducibility of the experimental findings.

To verify the reproducibility of the OGTT results shown in Figure 5e-g, the same rats that were tested with IPGTT were tested with OGTT 3 days later. As shown in Figure S9, there was a significant reduction in glucose response that was similar to the result in the rats tested only with OGTT shown in Figure 5e-g (Figure S9) supporting the reproducibility of LuCl's localized barrier effect.

#### 4. Randomization

Describe how samples/organisms/participants were allocated into experimental groups.

All the SD rats used in the study were acclimatized for at least one week with ad libitum access to standard rat chow and randomly allocated into different groups.

#### 5. Blinding

Describe whether the investigators were blinded to group allocation during data collection and/or analysis.

The investigators were not blinded to allocation during experiments and outcome assessment.

Note: all in vivo studies must report how sample size was determined and whether blinding and randomization were used.

## 6. Statistical parameters

For all figures and tables that use statistical methods, confirm that the following items are present in relevant figure legends (or in the Methods section if additional space is needed).

n/a Confirmed

- The exact sample size (*n*) for each experimental group/condition, given as a discrete number and unit of measurement (animals, litters, cultures, etc.)
- A description of how samples were collected, noting whether measurements were taken from distinct samples or whether the same sample was measured repeatedly
- A statement indicating how many times each experiment was replicated
- The statistical test(s) used and whether they are one- or two-sided  
*Only common tests should be described solely by name; describe more complex techniques in the Methods section.*
- A description of any assumptions or corrections, such as an adjustment for multiple comparisons
- Test values indicating whether an effect is present  
*Provide confidence intervals or give results of significance tests (e.g. *P* values) as exact values whenever appropriate and with effect sizes noted.*
- A clear description of statistics including central tendency (e.g. median, mean) and variation (e.g. standard deviation, interquartile range)
- Clearly defined error bars in all relevant figure captions (with explicit mention of central tendency and variation)

See the web collection on [statistics for biologists](#) for further resources and guidance.

## ► Software

Policy information about [availability of computer code](#)

### 7. Software

Describe the software used to analyze the data in this study.

All statistical analyses were performed with Prism® software (Version 7.0c, GraphPad Softwares Inc.).

For manuscripts utilizing custom algorithms or software that are central to the paper but not yet described in the published literature, software must be made available to editors and reviewers upon request. We strongly encourage code deposition in a community repository (e.g. GitHub). *Nature Methods* [guidance for providing algorithms and software for publication](#) provides further information on this topic.

## ► Materials and reagents

Policy information about [availability of materials](#)

### 8. Materials availability

Indicate whether there are restrictions on availability of unique materials or if these materials are only available for distribution by a third party.

No unique materials used

### 9. Antibodies

Describe the antibodies used and how they were validated for use in the system under study (i.e. assay and species).

No antibodies used.

### 10. Eukaryotic cell lines

a. State the source of each eukaryotic cell line used.

No eukaryotic cell line used

b. Describe the method of cell line authentication used.

No eukaryotic cell line used

c. Report whether the cell lines were tested for mycoplasma contamination.

No eukaryotic cell line used

d. If any of the cell lines used are listed in the database of commonly misidentified cell lines maintained by [ICLAC](#), provide a scientific rationale for their use.

No commonly misidentified cell lines were used.

## ► Animals and human research participants

Policy information about [studies involving animals](#); when reporting animal research, follow the [ARRIVE guidelines](#)

### 11. Description of research animals

Provide all relevant details on animals and/or animal-derived materials used in the study.

#### Animals

All the experimental animal protocols were approved by the Brigham and Women's Hospital Institutional Animal Care and Use Committee (IACUC). All animals received humane care in accordance with the 1996 "Guide for the care and use of laboratory animals" recommended by the US National Institutes of Health. Male Sprague-Dawley rats (Harlan, IN) were acclimatized under a 12:12 light: dark cycle (lights-on 7 AM) for at least one week with ad libitum access to standard rat chow. Experiments were performed after an overnight fast with access to water.

#### CT imaging of rats gavaged with LuCl or sucralfate

CT imaging was used to visualize the LuCl (or sucralfate) in gastrointestinal (GI) tract in rats. Briefly, the rats were gavaged with the hydrated LuCl pastes (or sucralfate suspension in 0.9w/v% normal saline) (dose: 450mg/kg rat). After predetermined time points (for example, 1, 5 or 24 hr), the rats were anesthetized using 3% isoflurane for 1 min and placed in CT with continuous anesthesia using 1% isoflurane throughout the imaging session. The CT imaging parameters are as followed; Current: 150 $\mu$ A, voltage: 40kV, number of projections: 360, shots: 4 shots (total imaging time: 7 min). The raw images were processed, restructured into different view axes (including 3-D projections and 3-D videos) and analyzed using ImageJ (1.48v, NIH).

#### Histological analysis of the intestine of rats gavaged with LuCl

To assess the impact of LuCl on epithelium, SD rats were gavaged with LuCl daily for 6 days and their GI tracts were harvested for histological assessments. Briefly, rats were fasted overnight before the first gavage day and gavaged with LuCl (n=3, 450mg/kg rat) or 0.9%w/v saline solution (n=3). The rats were fed with a normal diet and water ad libitum after the first gavage. From day 2 to day 6, rats were gavaged daily with LuCl or saline without fasting. on day 7, GI tracts were harvested, processed for histological assessments, and stained using haematoxylin and eosin (H&E) staining.

#### Oral glucose tolerance tests (OGTT) and intraperitoneal glucose tolerance tests (IPGTT)

To evaluate the in vivo effect of LuCl and sucralfate on postprandial glucose absorption or systemic absorption, SD rats were pre-gavaged with the hydrated LuCl pastes and subsequently had an OGTT or IPGTT. Considering the technical difficulties in gavaging the dry powder (i.e. animal discomfort, precise dosing), LuCl was hydrated with 0.9 %w/v saline solution right before the gavage. When the dry LuCl is hydrated as a 0.9 %w/v saline solution, the 450mg/kg rat dose for 400-500g rats (i.e. 180-225mg dose per rat) results in a paste volume of 0.7-0.9ml. For the higher 2,700mg/kg dose, the paste volume was 4.2-5.4ml. This dosing volume is in accordance with USDA guidelines, which allows up to 16ml (10-20ml/kg) for a 400g rat. In standard OGTT experiments, SD rats were fasted overnight (starting time: 7pm the prior day with access to water, duration of fast: 15 hr prior to treatment with LuCl) and gavaged with sucralfate, LuCl (dose: 450mg/kg rat), or saline in pre-determined dosing schedule. For High Dose (Figure 6a-b), a LuCl dose of 2,700mg/kg rat (6 times higher than the initial dose) was gavaged. Then, 0.5g/ml glucose solution at a dose of 2g/kg rat was gavaged one hour after the last gavage to measure changes in glucose levels for 120 min (n=4 at least per arm). Blood was collected from the tail vein to measure blood glucose level using a glucometer (OneTouch UltraSmart, LifeScan Inc., USA). All rats received both the saline and LuCl treatment but on different days. Each data point was plotted with time as the x-axis and incremental area under curve (iAUC) was calculated based on the plot and the pre-gavage glucose level as a baseline. Statistical significance was determined using one-way ANOVA. Results were considered significant when  $p \leq 0.05$ . In standard IPGTT experiments, SD rats were treated the same as in OGTT experiments except that the glucose solution (2g/kg rat) was injected into the peritoneum one hr after the last gavage of saline, or LuCl to measure the changes in glucose level for 120 min (n=4 at least per arm).

#### Fluorescence imaging of harvested rat GI tract with LuCl gavage

SD rats were gavaged with LuCl (dose: 450mg/kg rat) encapsulated with FITC-BSA (2w/w% in LuCl powder), and the GI tracts from stomach to cecum were harvested after 1hr or 24hr. The harvested GI tracts were imaged using IVIS Spectrum In Vivo Imaging System (Perkin Elmer). Rats without LuCl gavage were used as a control and all the images were normalized using the control.

Policy information about [studies involving human research participants](#)

### 12. Description of human research participants

Describe the covariate-relevant population characteristics of the human research participants.

The study did not involve human research participants.